Species	BOA (°)	GAPE (mm)	PMX (mm)	LJA (°)	HX (mm)	CR (°)	TTPG (ms)	TTPMX (ms)	TTPH (ms)	TTCR (ms)	TTJR (ms)
Bodianus bimaculatus	86.61	0.97	0.60	27.13	0.21	6.67	14.05	17.15	19.31	19.51	37.18
Bodianus rufus	76.51	1.03	1.30	20.43	0.19	4.23	14.08	16.13	18.32	18.35	33.51
Choerodon fasciatus	72.51	2.93	2.11	34.3	0.28	4.73	16.21	19.89	24.82	27.48	60.51
Coris gaimard	70.63	1.97	1.73	29.64	0.23	5.64	13.43	15.16	22.75	21.15	57.05
Diproctacanthus xanthurus	75.15	1.21	0.64	12.98	0.23	3.46	11.86	12.01	13.72	16.21	31.51
Halichoeres bivittatus	77.66	1.48	1.11	18.98	0.25	4.08	12.53	15.15	17.77	19.15	34.62
Halichoeres cyanocephalus	72.82	1.52	0.92	16.48	0.22	4.42	12.15	15.08	17.37	16.51	36.51
Halichoeres garnoti	77.98	2.04	1.04	31.09	0.19	3.83	14.41	14.89	20.55	23.05	46.15
Hemigymnus melapterus	66.99	2.67	1.43	31.65	0.19	5.21	14.10	16.09	22.29	23.51	48.88
Labroides dimidiatus	58.29	1.26	0.67	13.02	0.16	2.26	10.27	11.28	15.00	15.00	30.27
Labroides pectoralis	60.15	1.30	0.62	12.98	0.17	3.01	11.15	11.95	14.70	15.68	31.05
Larabicus quadrilineatus	64.14	1.41	0.38	11.69	0.26	3.49	11.17	11.00	16.20	16.10	32.28
Pseudojuloides cerasinus	86.15	1.56	1.35	33.20	0.22	5.46	14.86	18.15	22.02	20.61	48.15
Pseudocheilinus evanidus	86.43	1.46	1.83	27.56	0.25	4.91	15.16	17.16	20.64	22.13	39.84
Pseudocheilinus hexataenia	75.15	1.33	0.93	22.10	0.18	3.70	13.64	14.65	16.63	16.15	33.08
Thalassoma duperrey	75.15	3.06	2.22	28.94	0.24	4.88	15.15	20.15	27.72	28.08	56.54
Thalassoma hardwicke	88.51	3.92	2.72	35.07	0.28	7.56	16.68	24.98	23.67	26.08	63.51
Thalassoma jansenii	70.55	4.38	2.55	33.49	0.22	5.67	16.54	23.54	23.25	25.51	60.15
Thalassoma lutescens	70.02	3.11	2.22	25.88	0.25	4.56	14.78	21.76	25.48	25.54	55.90

Table S1 – Species' mean data. Mean values for kinematic and morphological variables for each species. Abbreviations: SL, standard length; MCA, area of the maxillary crest of the premaxilla; BOA, body orientation angle; GAPE, peak gape; PMX, peak premaxillary protrusion; LJA, peak lower jaw angle; HX, hyoid excursion distance; CR, peak cranial rotation; TTPG, time to peak gape; TTPMX, time to peak premaxillary protrusion; TTPH, time to peak hyoid excursion; TTCR, time to peak cranial rotation; TTJR, time to jaw retraction

Table S1 (contd.)

Species	SL (mm)	MCA (units^2)
Bodianus bimaculatus	38.44	836
Bodianus rufus	40.98	851
Choerodon fasciatus	63.70	1538
Coris gaimard	54.38	884
Diproctacanthus xanthurus	48.08	202
Halichoeres bivittatus	48.62	1070
Halichoeres cyanocephalus	48.51	1277
Halichoeres garnoti	64.06	628
Hemigymnus melapterus	43.25	838
Labroides dimidiatus	50.73	107
Labroides pectoralis	51.39	182
Larabicus quadrilineatus	42.86	181
Pseudojuloides cerasinus	64.91	1135
Pseudocheilinus evanidus	44.57	891
Pseudocheilinus hexataenia	39.06	510
Thalassoma duperrey	84.04	1392
Thalassoma hardwicke	77.70	1590
Thalassoma jansenii	76.47	1782
Thalassoma lutescens	73.93	1460

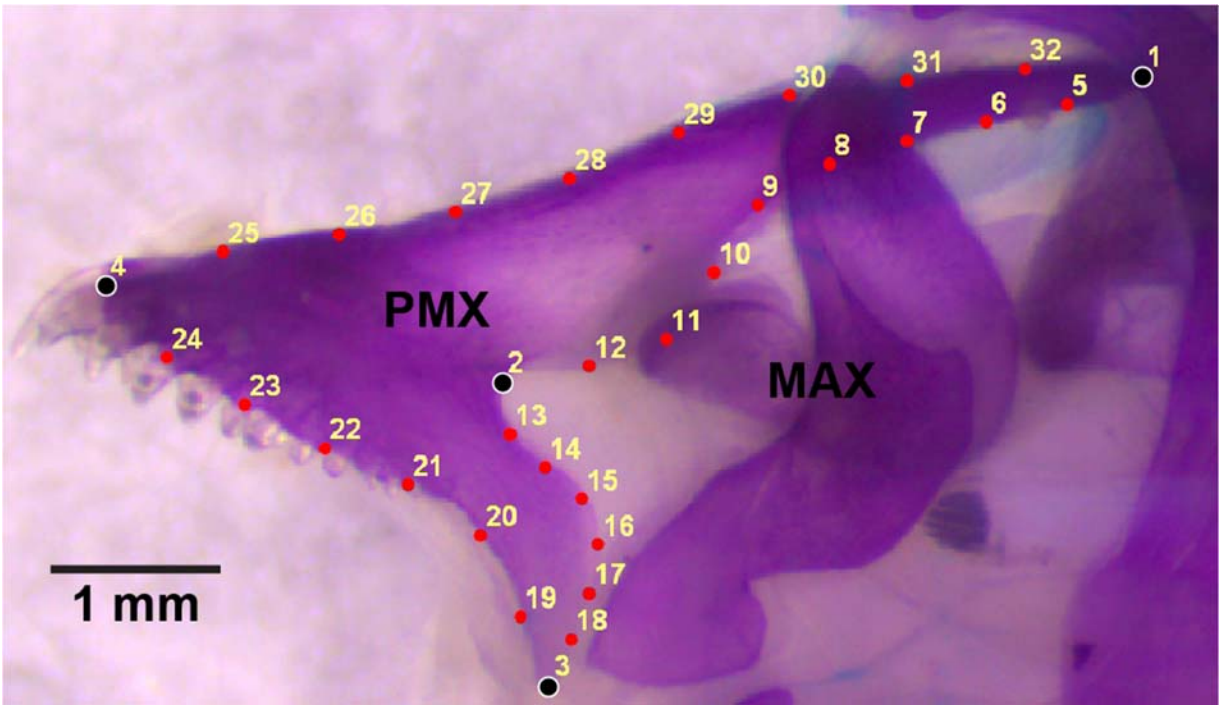

Fig. S1 – Digitization of premaxillary shape. Lateral images of the premaxilla of each specimen were imported into the program tpsDig2 (Rohlf 2006) for the placement of landmarks and semi-landmarks. Four landmarks (black) were placed on lateral photographs of each specimen, labeled as 1-4 in the figure. The landmarks were: (1) the distal end of the ascending process, (2) the intersection of the ascending and alveolar processes, (3) the distal end of the alveolar process, and (4) the root of the anteriormost caniform tooth. Twenty-eight additional semi-landmarks (red) distributed across 4 separate curves were placed along the outline of the bone (numbered 5-32 in the figure). Not shown are curves along which semi-landmarks could slide.

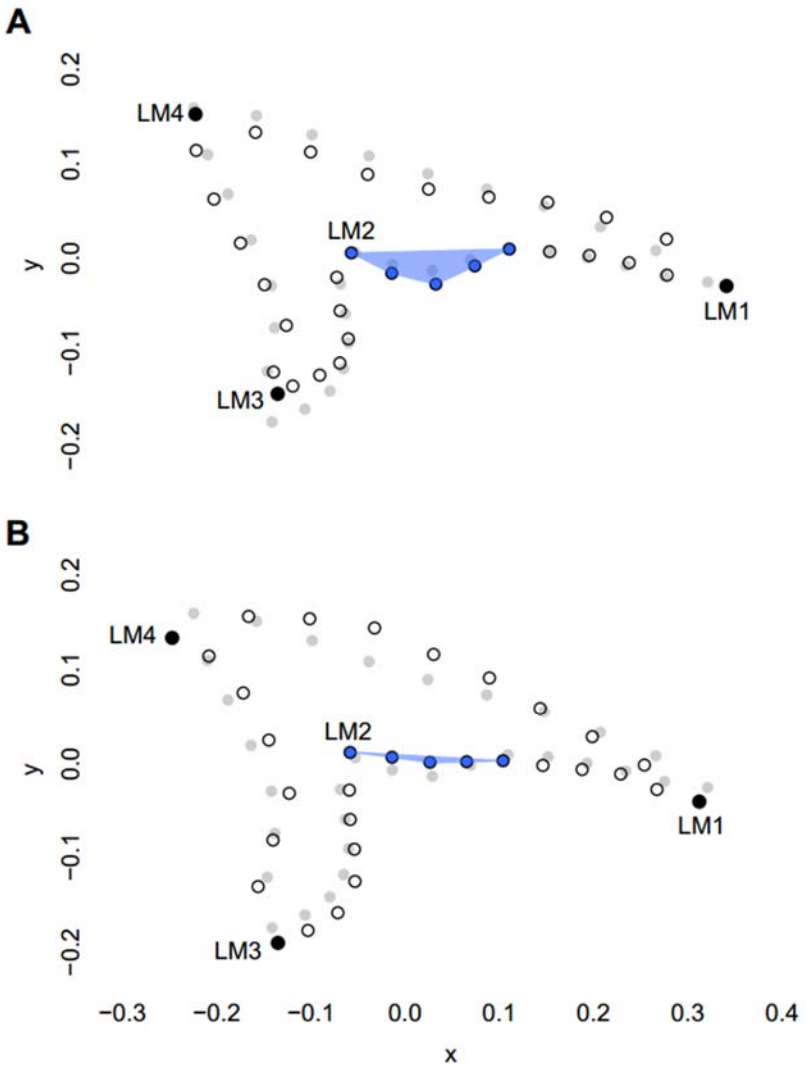

Fig. S2 – Measurement of the area of the maxillary crest. After species' mean premaxillary landmark sets were Procrustes superimposed, coordinate data were imported into the program ImageJ. The area of the maxillary crest on the premaxilla was captured by the points in blue: landmark 2 (LM2) and the next four semi-landmarks along the ventral edge of the ascending process. The area of the polygon contained within these five points was taken as a close approximation of the area of the maxillary crest. Shown above are mean landmarks for A) *Thalassoma hardwicke* and B) *Larabicus quadrilineatus*. Black, filled circles correspond to landmarks (except LM2), while open circles represent semi-landmarks (except those that capture the crest). Grey filled circles in the background of each panel show the mean shape across all species.

(Size-Corrected) Kinematic Variable	Model	ΔAICc	Slope (s.e.)	Intercept (s.e.)	Additional Parameters
Time to Peak Premaxillary Protrusion	OLS	0	0.0041 (0.0008)	-4.6946 (0.8627)	-
	PGLS – BM	8.00	0.0044 (0.0011)	-4.2969 (1.9430)	$\gamma = 1.00$
	PGLS – Pagel	1.58	0.0041 (0.0009)	-4.1632 (1.0871)	$\lambda = 0.46$
	PGLS – OU	1.67	0.0041 (0.0008)	-4.6904 (0.8613)	$\alpha = 0.46$
Peak Premaxillary Protrusion	OLS	0	0.0011 (0.0002)	-1.0441 (0.1613)	-
	PGLS – BM	5.33	0.0006 (0.0002)	-0.6037 (0.3375)	$\gamma = 1.00$
	PGLS – Pagel	0	0.0011 (0.0002)	-1.0441 (0.1613)	$\lambda = 0.00$
	PGLS – OU	1.81	0.0010 (0.0001)	-0.9352 (0.1730)	$\alpha = 0.09$
Time to Jaw Retraction	OLS	0	0.0085 (0.0027)	-10.4579 (2.8581)	-
	PGLS – BM	3.47	0.0044 (0.0034)	-4.3672 (5.7082)	$\gamma = 1.00$
	PGLS – Pagel	0	0.0085 (0.0027)	-10.4579 (2.8581)	$\lambda = 0.00$
	PGLS – OU	1.70	0.0080 (0.0032)	-8.7515 (3.3363)	$\alpha = 0.09$

Table S2 – Comparisons of linear models fit to kinematic variables against maxillary crest area. The kinematic variable listed in the first column was used as the dependent variable in separate regressions against maxillary crest area (see Figure 7 for scatter plots). Four linear models were fit to each bivariate set: ordinary least squares and three phylogenetic generalized least squares (PGLS) models. All PGLS models were informed by the MCC phylogeny. Models were compared using AICc scores. Abbreviations: OLS – ordinary least-squares; PGLS – phylogenetic generalized least squares; BM – Brownian motion; OU – Ornstein-Uhlenbeck

(Size-Corrected) Kinematic Variable	Mean Difference	F-Ratio	p-value	Corrected p-value
Body Orientation Angle	-7.980	2.123	0.128 (0.115-0.176)	0.128 (0.115-0.176)
Peak Cranial Rotation	**-1.711**	**9.021**	**0.004 (0.003-0.009)**	**0.009 (0.008-0.014)**
Peak Lower Jaw Angle	**-13.112**	**21.969**	**0.001 (0.001-0.001)**	**0.005 (0.005-0.005)**
Peak Gape Distance	-0.695	2.826	0.084 (0.078-0.108)	0.095 (0.089-0.119)
Peak Premaxillary Protrusion	**-0.515**	**4.301**	**0.043 (0.028-0.050)**	**0.044 (0.029-0.051)**
Peak Hyoid Excursion	-0.006	0.376	0.536 (0.351-0.616)	0.525 (0.351-0.616)
Time to Peak Gape	**-2.082**	**10.462**	**0.003 (0.001-0.007)**	**0.009 (0.007-0.015)**
Time to Peak Premaxillary Protrusion	**-2.845**	**5.409**	**0.023 (0.017-0.034)**	**0.035 (0.029-0.046)**
Time to Peak Hyoid Excursion	**-2.646**	**5.660**	**0.017 (0.012-0.021)**	**0.031 (0.020-0.042)**
Time to Peak Cranial Rotation	**-3.520**	**7.300**	**0.009 (0.009-0.015)**	**0.016 (0.016-0.022)**
Time to Jaw Retraction	**-10.382**	**21.084**	**0.001 (0.001-0.003)**	**0.004 (0.004-0.007)**

Table S3 – Phylogenetic ANOVAs of kinematic data. Phylogenetic ANOVA was performed for each variable listed in the first column to compare mean data between cleaners and non-cleaners. To account for phylogenetic uncertainty, the MCC phylogeny and 100 additional phylogenies from the posterior distribution of Baliga and Law (2016) were used (separately) to perform analyses. Exploratory analyses revealed each variable to be positively correlated with standard length except for: body orientation angle and maximum cranial rotation. The size-influenced data were thus size-corrected using standard length following Revell (2009). Shown in each cell are results from the ANOVA using the MCC tree with ranges for additional analyses in parentheses (values for Mean Difference and F-Ratios were nearly invariant and are thus not shown). Mean Difference was calculated by subtracting non-cleaner data from cleaner data; negative values thus indicate cleaner fishes possess smaller trait magnitudes on average. In the final column, p-values are corrected using methods from Benjamini and Hochberg (1995) to control the false discovery rate. Bold rows indicate significant differences between cleaners and non-cleaners.

Supplementary Movies

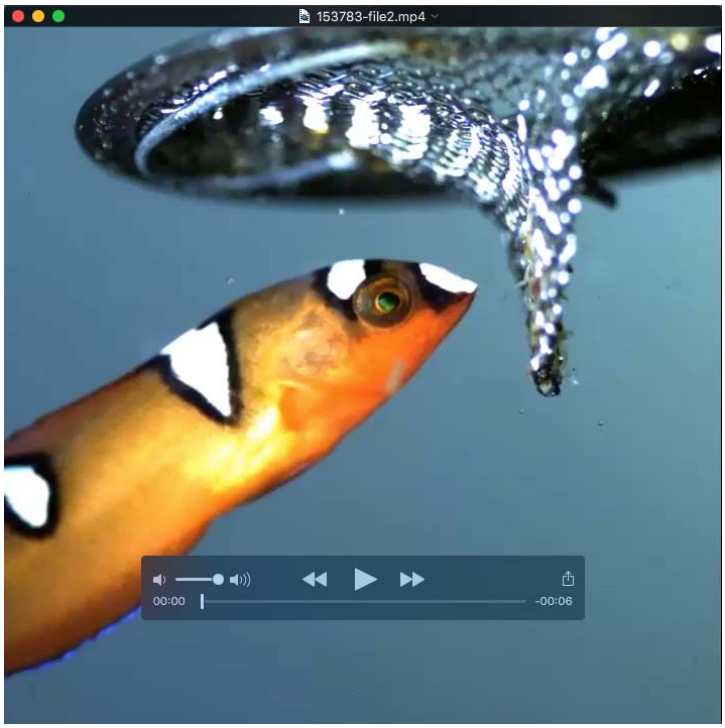

Movie 1 – *Coris gaimard* feeding on attached invertebrates and exhibiting a 'premaxillary bite'.

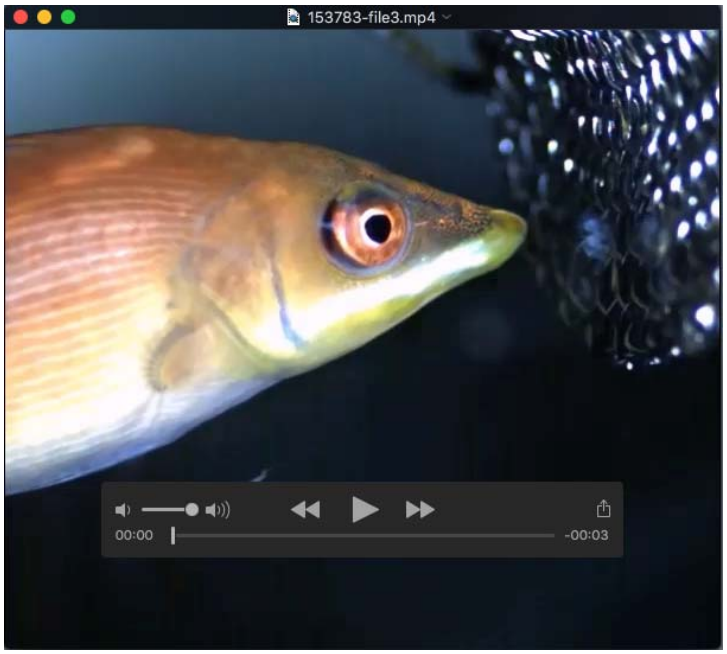

Movie 2 – *Pseudocheilinus evanidus* feeding on attached invertebrates and exhibiting a 'premaxillary bite'.

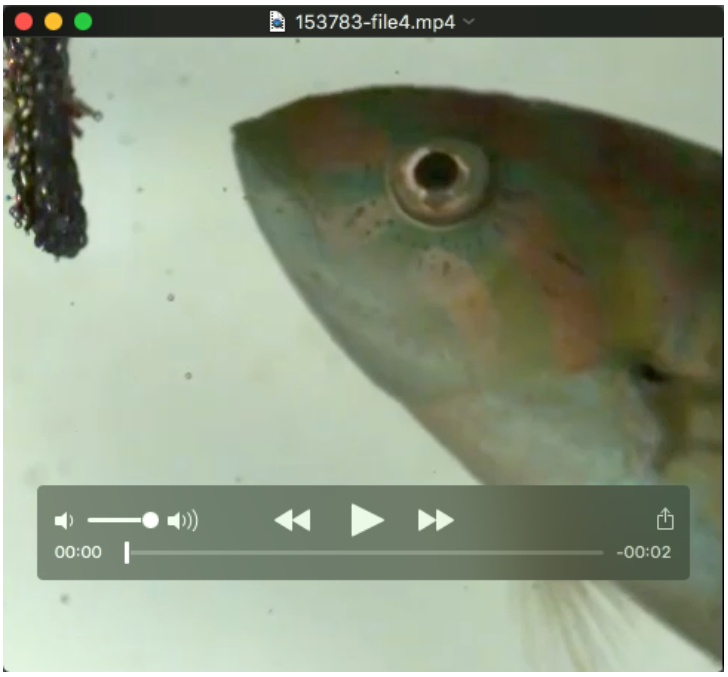

Movie 3 – *Thalassoma hardwicke* feeding on attached invertebrates and exhibiting a 'premaxillary bite'.

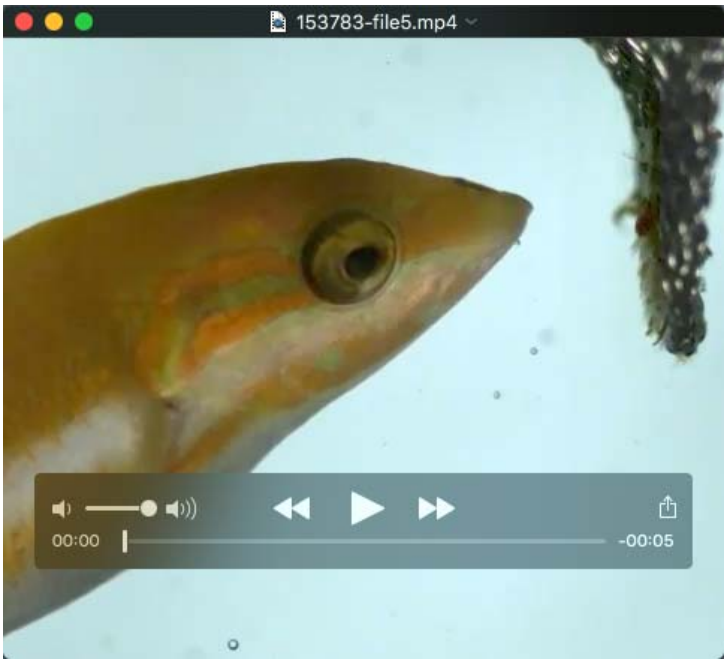

Movie 4 – *Thalassoma lutescens* feeding on attached invertebrates and exhibiting a 'premaxillary bite'.

Movie 5 – *Labroides dimidiatus* feeding on attached invertebrates. No rapid anteroventral decent of the premaxilla is apparent as the bite is delivered.

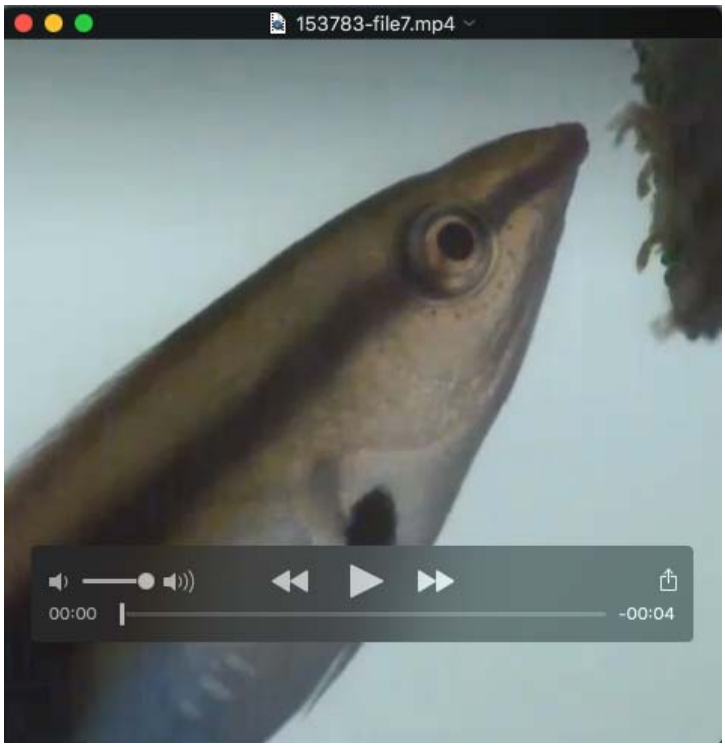

Movie 6 – *Labroides pectoralis* feeding on attached invertebrates. No rapid anteroventral decent of the premaxilla is apparent as the bite is delivered.